

# Revisiting Imidazolium Based Ionic Liquids: Effect of the Conformation Bias of the [NTf<sub>2</sub>] Anion Studied By Molecular Dynamics Simulations

Benjamin Golub,<sup>1,\*</sup> Jan Neumann,<sup>1,†</sup> Lisa-Marie Odebrecht,<sup>1,‡</sup> Ralf Ludwig,<sup>2,3,§</sup> and Dietmar Paschek<sup>1,¶</sup>

<sup>1</sup>*Institut für Chemie, Abteilung Physikalische und Theoretische Chemie, Universität Rostock, Albert-Einstein-Straße 21, D-18059 Rostock, Germany*

<sup>2</sup>*Institut für Chemie, Abteilung Physikalische und Theoretische Chemie, Universität Rostock, Dr.-Lorenz-Weg 2, D-18059 Rostock, Germany*

<sup>3</sup>*Leibniz Institut für Katalyse an der Universität Rostock, Albert-Einstein-Straße 29a, D-18059 Rostock, Germany*

(Dated: August 1, 2018)

We study ionic liquids composed 1-alkyl-3-methylimidazolium cations and bis(trifluoromethylsulfonyl)imide anions ([C<sub>n</sub>MIm][NTf<sub>2</sub>]) with varying chain-length  $n = 2, 4, 6, 8$  by using molecular dynamics simulations. We show that a reparametrization of the dihedral potentials as well as charges of the [NTf<sub>2</sub>] anion leads to an improvement of the force field model introduced by Köddermann *et al.* [ChemPhysChem, **8**, 2464 (2007)] (KPL-force field). A crucial advantage of the new parameter set is that the minimum energy conformations of the anion (*trans* and *gauche*), as deduced from *ab initio* calculations and RAMAN experiments, are now both well represented by our model. In addition, the results for [C<sub>n</sub>MIm][NTf<sub>2</sub>] show that this modification leads to an even better agreement between experiment and molecular dynamics simulation as demonstrated for densities, diffusion coefficients, vaporization enthalpies, reorientational correlation times, and viscosities. Even though we focused on a better representation of the anion conformation, also the alkyl chain-length dependence of the cation behaves closer to the experiment. We strongly encourage to use the new NGKPL force field for the [NTf<sub>2</sub>] anion instead of the earlier KPL parameter set for computer simulations aiming to describe the thermodynamics, dynamics and also structure of imidazolium based ionic liquids.

## INTRODUCTION

Having a reliable force field available is one of the most important prerequisites for setting up a molecular dynamics simulation. Hence, a lot of effort has been put into the development of new as well as the improvement of existing force field models. There are essentially two different approaches on how to improve or optimize force fields:

One approach is trying to develop a “universal” force field parameter set which can be applied to a broad range of different molecules or ions, such as the force field parameters for ionic liquids introduced by Pádua *et al.* [1–10]. These force fields are very popular in the ionic liquids molecular simulation community and yield in general good results in comparison with experimental data.

An alternative, less universal approach is to focus on a specific subset of molecules and ions, and to enhance the quality of the model by fitting the parameters of a system to a set of selected thermodynamical, dynamical and structural properties, which then can be accurately emulated by the force field. The most well-known example for the application of such a strategy is perhaps the water molecule. In 2002 Bertrand Guillot gave a comprehensive overview over (at the time) more than 40 different water models [11], and the number has been increasing since then [12–15]. Obviously, water is of great scientific interest. As a consequence, there exist a variety of force field models consisting mostly of three (SPC, TIP3P) to five (TIP5P, ST2) interaction sites, including (POL5) or without (SPC/E) polarizability and even

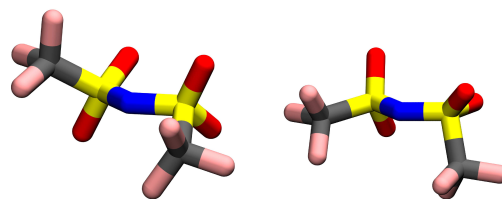


FIG. 1. Minimum energy conformations of the [NTf<sub>2</sub>] anion taken from a MD simulation employing the KPL force field.

force fields optimized to best represent the solid phases of water (TIP4P/ICE) and their phase transitions.

The second strategy was employed by Köddermann *et al.* in 2007 to arrive at the KPL (Köddermann, Paschek, Ludwig) force field for a selected class of imidazolium based ionic liquids composed of 1-alkyl-3-methylimidazolium cations and bis(trifluoromethylsulfonyl)imide anions ([C<sub>n</sub>MIm][NTf<sub>2</sub>]) [16]. Aim of this work was to further optimize the force field of Pádua *et al.* to better represent dynamical properties like self-diffusion coefficients, reorientational correlation times, and viscosities. As shown in their original work from 2007 as well as in further works published by different groups, the KPL force field has been proven to yield reliable results for dynamical properties, but also thermodynamical properties, such as the free energies of solvation for light gases in ionic liquids [17, 18], and is still used frequently to this date [19–21].

Here we want to present our take on further improving the KPL force field by revisiting the conformation-

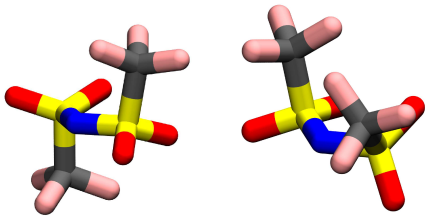


FIG. 2. Minimum energy conformations of the  $[\text{NTf}_2]$  anion obtained from *ab initio* calculations. The *trans* conformation (left) represents the global energy minimum, while the energy of the *gauche* conformation (right) is elevated by about  $3 \text{ kJ mol}^{-1}$ .

space explored by the  $[\text{NTf}_2]$  anion. Extensive studies of the conformation of the  $[\text{NTf}_2]$  anion using the KPL force field in comparison to experimental as well as quantum chemical calculations have revealed a significant mismatch of the energetically favored conformations. Therefore we feel the need for presenting a modified version of the force field, removing this conformation-bias. We are discussing the implications of this modification for a wealth of thermodynamical, dynamical, and structural quantities.

### CONFORMATION-SPACE OF THE ANION

During MD simulations of ionic liquids of the type  $[\text{C}_n\text{MIm}][\text{NTf}_2]$  with the force field of Köddermann *et al.* it became apparent that the favored  $[\text{NTf}_2]$  anion conformations observed in the simulation differ from what has been shown earlier from quantum chemical calculations [6] as well as from RAMAN experiments [22] (see Fig. 1 and Fig. 2).

For locating the minimum energy conformations we performed extensive quantum chemical calculations with the GAUSSIAN 09 program [23] following the approach of Pádua *et al.* [2]. We started by calculating the potential energy surface as a function of the two dihedral angles S1-N-S2-C2 ( $\phi_1$ ) and S2-N-S1-C1 ( $\phi_2$ ) on the HF level with a small basis set (6-31G\*). Subsequent to these optimizations we performed single point calculations on the MP2 level using the cc-pvtz basis set for all HF optimized conformations. In agreement with earlier calculations by Pádua *et al.* [6], and RAMAN measurements of Fujii *et al.* [22], we observe essentially two structurally distinct minimum energy conformations that can be identified as energy minima on the energy-landscape depicted in Fig. 3. The *trans* conformations of the  $[\text{NTf}_2]$  anion are energetically preferred, followed by the *gauche*-conformations, which are elevated by about  $3 \text{ kJ mol}^{-1}$  (see Fig. 2).

To compare these *ab initio* calculations with the KPL force field model, we employed the molecular dynamics package MOSCITO 4.180 and computed the same potential energy surface as a function of the two dihedral

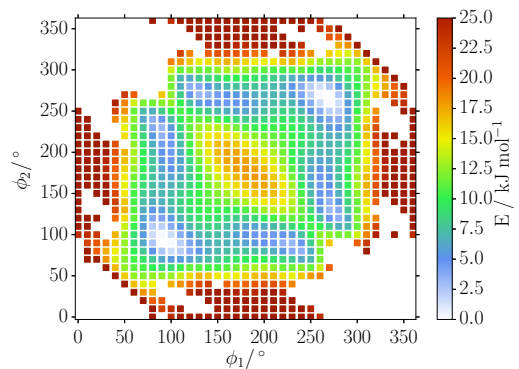


FIG. 3. *Ab initio* computation of the energy surface of the  $[\text{NTf}_2]$  anion as a function of the S1-N-S2-C2, and S2-N-S1-C1 dihedral angles  $\phi_1$  and  $\phi_2$ .

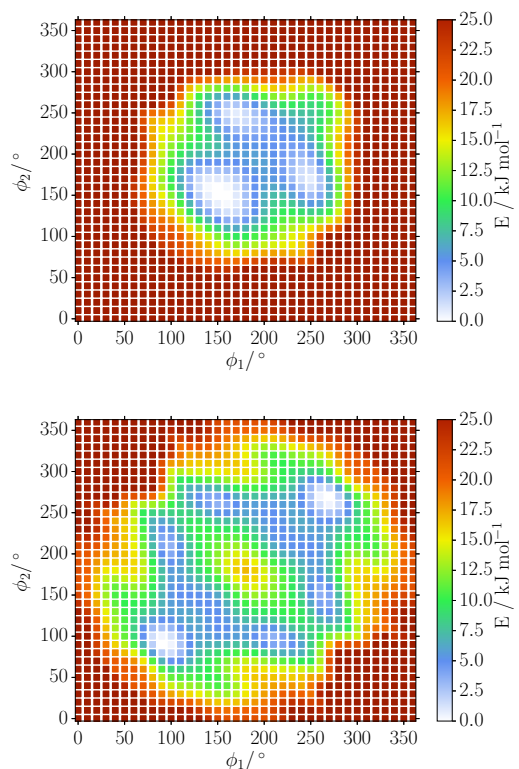


FIG. 4. Potential energy surface of the  $[\text{NTf}_2]$  anion computed for the two force field models. The new force field (bottom panel) provides a much better representation of the *ab initio* calculations shown in Fig. 3 than the the original KPL force field (top panel).

angles  $\phi_1$  and  $\phi_2$  (see Fig. 4 top panel) by fixing the two dihedral angles and optimizing all other degrees of freedom. We would like to add that in the force field-optimizations all bond-lengths were kept fixed. It is quite obvious that the KPL force field does not adequately reproduce the potential energy surface obtained from the

quantum chemical calculations (compare the top panel in Fig. 4 with FIG 3). The minimum energy conformations of the KPL model reveals essentially two structurally distinct conformations illustrated in Fig. 1. However, both are somewhat similar, being positioned between the *trans* and *gauche* conformations favoured in the *ab initio* calculations. The fact that the energy landscape does not reflect all the symmetry-features of the molecule, however, might be a lesser problem since energy barriers are rather large and the anion could explore similar conformations simply by rotation.

However, for arriving at a better representation of the *ab initio* energy surface, we reparameterized the charges as well as the two distinct independent dihedral potentials (S-N-S-C and F-C-S-N), while keeping the other parameters unchanged. From our quantum chemical calculations we yield the global minimum conformations at  $\phi_1 = \phi_2 = 90^\circ$  and  $\phi_1 = \phi_2 = 270^\circ$ . Due to the symmetry of the [NTf<sub>2</sub>] anion these two minima are conformationally identical. To calculate the parameters for the S-N-S-C dihedral angle, we fixed  $\phi_1$  at  $90^\circ$  and calculated the energy as function of the dihedral angle  $\phi_2$  on the MP2 level using a cc-pvtz basis set (as shown in Fig. 5). The same procedure was applied using the KPL force field while switching of the dihedral potential, such that only the nonbonding (nb) interactions matter. We then subtracted the latter energy function from the energies obtained via the QM calculations, and arrive at the dihedral potential for the dihedral angle S-N-S-C, which should be reproduced by the torsion potential in our force field (see Fig. 5 bottom panel).

In contrast to Köddermann *et al.*, we chose to fit a dihedral potential function obeying the conformational symmetry-features of the anion using

$$V_{\kappa\lambda\omega\tau}^{\text{dp}} = \sum_n k_m^{\text{dp}} [1 + \cos(m_n \psi_m - \psi_m^0)] \quad (1)$$

(with  $n = 6$  and  $\psi_m^0 = 0$ ) to the computed *ab initio* potential, leading to the proper minimum energy conformations of the [NTf<sub>2</sub>] anion [2]. Similarly obtained were parameters for the F-C-S-N dihedral potential of the terminal CF<sub>3</sub>-groups (see Fig. 6). The complete set of new parameters for the NGKPL force field is given in Table III. All charges were computed from the MP2-wavefunction using the method of Merz and Kollman as implemented in in the GAUSSIAN 09 programm. [24]. The refined charges are listed in Table I.

Finally, employing new refined parameters for the dihedral potentials and partial charges, we re-calculated the energy surface as a function of the two dihedral angles  $\phi_1$  and  $\phi_2$  (see Fig. 4 bottom panel). The result is in much better agreement with the *ab initio* calculations and resolves the conformational mismatch issue for the force field of the [NTf<sub>2</sub>] anion.

All parameters for the new [NTf<sub>2</sub>] anion force field are listed in the Tables I-III. The original parameters as well

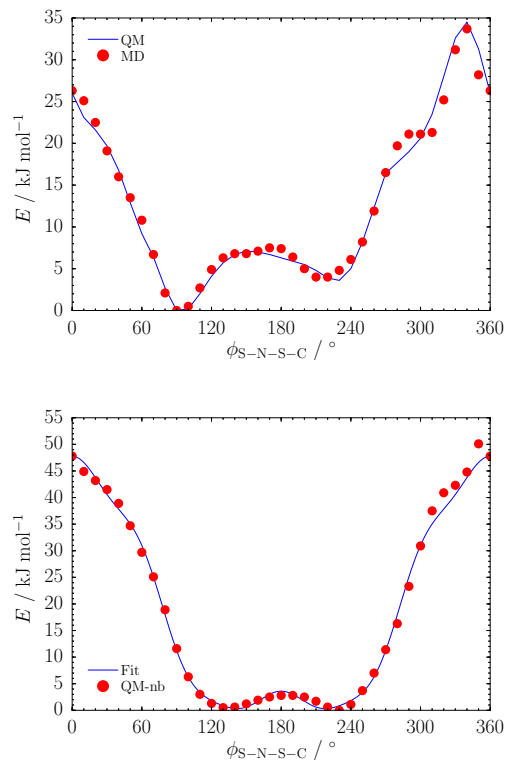


FIG. 5. Top panel: Potential energy of the entire [NTf<sub>2</sub>] anion as a function of the of S2-N-S1-C1 dihedral angle  $\phi_2$  with  $\phi_1$  being fixed at  $\phi_1 = 90^\circ$ . Bottom panel: Torsion potential fitted to the difference between QM and force field model (with switched off torsion potential).

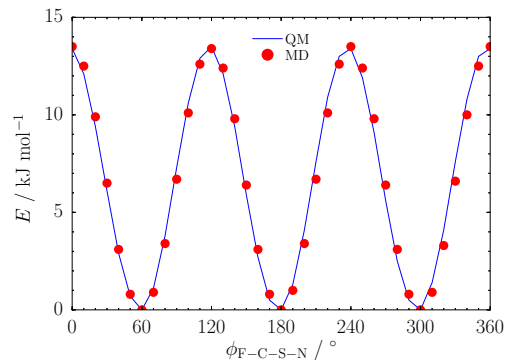


FIG. 6. Potential energy of the [NTf<sub>2</sub>] anion as function of the F-C-S-N dihedral angle.

as the parameters for the cations can be found in the publication of Köddermann *et al.* [16].

TABLE I. LENNARD-JONES parameters  $\sigma$ ,  $\epsilon$  and charges  $q$  for all interaction sites of the [NTf<sub>2</sub>] anion.

site	$\sigma / \text{\AA}$	$\epsilon / \text{K}$	$q / e$
F	2.6550	8.00	-0.189
C	3.1500	9.96	0.494
S	4.0825	37.73	1.076
O	3.4632	31.70	-0.579
N	3.2500	25.66	-0.690

TABLE II. Bond length  $r_{\kappa\lambda}^0$  and angle parameters  $\phi_{\kappa\lambda\omega}^0$  and  $k_{\kappa\lambda\omega}^a$  for the angle potential  $V_{\kappa\lambda\omega}^a = \frac{1}{2}k_{\kappa\lambda\omega}^a(\phi_{\kappa\lambda\omega} - \phi_{\kappa\lambda\omega}^0)^2$  in the force field of the [NTf<sub>2</sub>] anions.

bond	$r_{\kappa\lambda}^0 / \text{\AA}$	angle	$\phi_{\kappa\lambda\omega}^0 / ^\circ$	$k_{\kappa\lambda\omega}^a / \text{kJ mol}^{-1}\text{rad}^{-2}$
C-F	1.323	F-C-F	107.1	781.0
C-S	1.818	S-C-F	111.8	694.0
S-O	1.442	C-S-O	102.6	870.0
N-S	1.570	O-S-O	118.5	969.0
		O-S-N	113.6	789.0
		C-S-N	100.2	816.0
		S-N-S	125.6	671.0

## MOLECULAR DYNAMICS SIMULATIONS

We performed MD simulations for the two force fields KPL and NGKPL with GROMACS 5.0.6 [25–29] over a temperature range from  $T = 273 - 483$  K to calculate thermodynamical and dynamical properties and compare them with the original KPL force field. All simulations were carried out in the  $NpT$  ensemble. However, to compute viscosities, we performed additional  $NVT$  simulations using starting configurations sampled along the  $NpT$ -trajectory. Periodic boundary conditions were applied using cubic simulation boxes containing 512 ion-pairs. We applied smooth particle mesh EWALD summation [30] for the electrostatic interactions with a real space cutoff of 0.9 nm, a mesh spacing of 0.12 nm and 4th order interpolation. The EWALD convergence factor

TABLE III. Parameters  $k_m^{\text{dp}}$  and  $\psi_m^0$  for the torsion potential  $V_{\kappa\lambda\omega\tau}^{\text{dp}} = \sum_n k_m^{\text{dp}} [1 + \cos(m_n\psi_m - \psi_m^0)]$  in the force field of the [NTf<sub>2</sub>] anion.

	$n(\kappa\lambda\omega\tau)$	$m_n$	$k_m^{\text{dp}} / \text{kJ mol}^{-1}$	$\psi_m^0 / ^\circ$
F-C-S-N	1	3	2.0401	0.0
S-N-S-C	1	1	23.7647	0.0
	2	2	6.2081	0.0
	3	3	-2.3684	0.0
	4	4	-0.0298	0.0
	5	5	0.6905	0.0
	6	6	1.0165	0.0

$\alpha$  was set to  $3.38 \text{ nm}^{-1}$  (corresponding to a relative accuracy of the EWALD sum of  $10^{-5}$ ). All simulations were carried out with a timestep of 2.0 fs, while keeping bond lengths fixed using the LINCS algorithm [31].

An initial equilibration was done for 2 ns at  $T = 500$  K applying BERENDSEN thermostat as well as BERENDSEN barostat with coupling times  $\tau_T = \tau_p = 0.5$  ps [32]. After this another equilibration was done for 2 ns at each of the desired temperatures. For each of the six temperatures 273 K, 303 K, 343 K, 383 K, 423 K and 483 K we performed production runs of 30 ns, keeping the the pressure fixed at 1 bar applying NOSÉ-HOOVER thermostats [33, 34] with  $\tau_T = 1$  ps and RAHMAN-PARRINELLO barostats [35, 36] with  $\tau_p = 2$  ps.

## RESULTS & DISCUSSION

Analogous to the publication of Köddermann *et al.* from 2007 [16] we will compare densities, self-diffusion coefficients and vaporization enthalpies for [C<sub>n</sub>MIm][NTf<sub>2</sub>] as function of temperature and alkyl chain-length as well as viscosities and reorientational correlation times for [C<sub>2</sub>MIm][NTf<sub>2</sub>] as function of temperature. It is important to keep in mind, that the original force field was optimized to reproduce these properties and yields a good agreement between experiment and simulation. By resolving the mismatch of the favored conformations of the [NTf<sub>2</sub>] anion we are able to describe these properties as good as the KPL force field or even better.

### Structural Features

Here we take a look at structural features of the liquid phase and in how they are influenced by changes in the conformation-population of the [NTf<sub>2</sub>] anion. First we inspect the three distinct center of mass pair distribution functions between the different ions computed for [C<sub>n</sub>MIm][NTf<sub>2</sub>] with  $n = 2$  at  $T = 303$  K (shown in Fig. 7). It is quite apparent that these distribution functions are only slightly affected by the alterations in the force field. Most notable are the differences observed in the anion-anion pair distribution function depicted in Fig. 7c with the first peak being significantly broadened. It is quite obvious to assume that this behavior is related to the more distinct conformational states (*trans* and *gauche*) that the reparameterized [NTf<sub>2</sub>] anion is adopting as shown in Fig. 2. In the *trans* state the molecule is more elongated along the molecular axis and more compact perpendicular to it. In addition, the *gauche*-state is generally more compact than the minimum energy conformations adopted by the original KPL force field model shown in Fig. 1. This leads to an enhanced population of both, short and long anion-anion distances. This effect manifests itself also in the slight shift of the max-

imum of the first peak of the anion-cation pair distribution function towards smaller distances (see Fig. 7a). Another interesting distribution function is the pair distribution function of the anion-oxygens surrounding the C(2)-hydrogen site on the cation. The C(2)-position is deemed to act as a hydrogen-bond donor [37, 38]. With changing conformations we expect an effect on the hydrogen bonding situation between the anion and cation. Here we observe that the NGKPL force field promotes hydrogen bonds between anions and cations as indicated by an increased first peak of the O-H pair distribution function shown in Fig. 8. The computed number of hydrogen bonds increases throughout by about 4 %, mostly unaffected by the alkyl chain-length and temperature (not shown). Taking into account the importance of more elongated *trans* configurations of the anion, it is also not surprising that the second peak is somewhat depleted, while the third peak is again enhanced (see Fig. 8). We further investigate the hydrogen-bond situation by not just looking at the distance between the oxygen and hydrogen, but also at the angular distribution. Therefore we compute the probability density map of the anion-oxygens surrounding the C(2) hydrogen site on the cation. Again we focus on the C(2) hydrogen because its hydrogen-bond interaction with the anion is deemed the strongest and most important. To calculate this map we compute both, the O-H distance as well as angle between the C-H bond-vector on the cation and the intermolecular C-O vector, where C is the C(2)-position of the cation and O represents the oxygen-sites on the anions. In addition, the computed probabilities are weighted by  $r_{\text{OH}}^{-2}$ . It is revealed that the maximum of this probability density map does not quite represent a linear hydrogen bond at a distance of 2.3 Å, but is tilted by about 25°, and is characterized by a rather broad angular distribution. (Fig. 9).

### Densities & Self-Diffusion Coefficients

To get an idea on how the changing conformation-populations influence the properties of the imidazolium based ionic liquids, we first take a look at the mass density of [C<sub>2</sub>MIm][NTf<sub>2</sub>]. In molecular simulations the density has always been an important property for evaluating a force field. The enhanced conformational diversity of the [NTf<sub>2</sub>] anion leads to a slight increase in the density over the whole temperature range (see Fig.10). This overall increase is in better agreement with the experimental data from Tokuda *et al.* [39]. For lower temperatures the NGKPL force field even matches the experimental values. The thermal expansivity, however, is significantly overestimated, although at the highest temperatures the difference between experiment and simulation is still within about 5 %. Despite the overall density increase from KPL to NGKPL, the thermal expansivities of both models are

TABLE IV. Temperature dependence of the density  $\rho$  and the self-diffusion coefficients of the [NTf<sub>2</sub>] anion  $D_-$  in [C<sub>2</sub>MIm][NTf<sub>2</sub>] according to the KPL and NGKPL force fields. See also Fig. 10 and Fig. 11.

$T / \text{K}$	$\rho / \text{kg m}^{-3}$		$D_- / 10^{-11} \text{ m}^2 \text{ s}^{-1}$	
	KPL	NGKPL	KPL	NGKPL
273	1525	1540	1.4	1.1
303	1485	1500	4.8	3.6
343	1433	1448	13.0	10.9
383	1383	1398	26.4	23.0
423	1335	1349	49.4	43.6
483	1265	1280	92.7	90.0

practically identical.

With this increasing density, also slightly reduced self-diffusion coefficients for the [NTf<sub>2</sub>] anion are observed (see Fig. 11). We calculated the self-diffusion coefficient using the EINSTEIN relation

$$D = \frac{1}{6} \lim_{t \rightarrow \infty} \frac{d}{dt} \langle |\vec{r}_i(t) - \vec{r}_i(0)|^2 \rangle \quad (2)$$

as function of the temperature for [C<sub>2</sub>MIm][NTf<sub>2</sub>] (Fig. 11) as well as as function of the alkyl chain-length of [C<sub>*n*</sub>MIm][NTf<sub>2</sub>] at  $T = 303 \text{ K}$  (Fig. 12). As shown in 2007 the KPL force field is able to yield self-diffusion coefficients in good agreement with the experimental data. Nevertheless, using the new NGKPL parameters we are able to describe the temperature dependence of the self-diffusion coefficient of the [NTf<sub>2</sub>] anion in [C<sub>2</sub>MIm][NTf<sub>2</sub>] even better (Fig. 11). Taking a look at the alkyl chain-length dependence we can support the findings for the  $n = 2$  imidazolium ionic liquid. The NGKPL force field is able to reproduce the dependence better, especially for  $n \leq 4$ , for longer chains the KPL force field is closer to the experiment (see Fig. 12). As observed for the temperature dependence the general trend of the self-diffusion coefficient as function of the alkyl chain-length is identical for the KPL and NGKPL force field.

### Vaporization Enthalpies

The magnitude of the vaporization enthalpy of ionic liquids was studied extensively over the last few years and has been sometimes discussed quite emotionally [40–48]. For the purpose of this study we will compare our results with the more recent QCM data of imidazolium based ILs of type [C<sub>*n*</sub>MIm][NTf<sub>2</sub>] from Verevkin *et al.* of 2013 [47] as shown in Fig. 13. We would like to point out that an exhaustive overview of the huge amount of vaporization enthalpy data from different experiments as well as molecular simulation studies is provided in the supporting informations of Verevkin *et al.* [47] and in the COSMOS-RS study by Schröder and Coutinho [48]. The

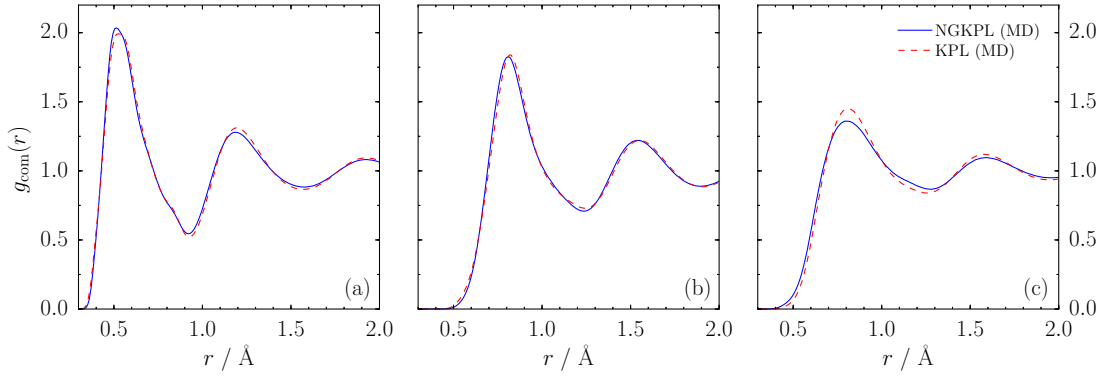


FIG. 7. Center of mass radial pair distribution functions for cation-anion (a), anion-anion (b) and cation-cation (c) for  $[\text{C}_2\text{MIm}][\text{NTf}_2]$  at  $T = 303$  K. The NGKPL-data are shown as blue lines and the KPL-data force as red dashed lines.

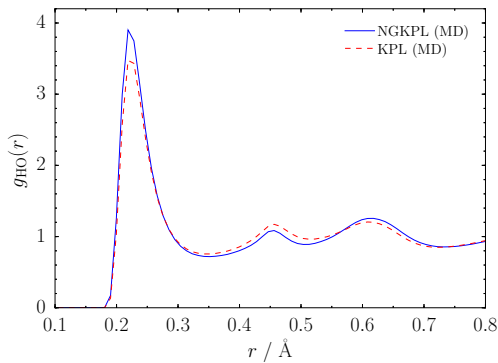


FIG. 8. Radial pair distribution function of the anion-oxygens around the C(2) hydrogen site on the cation for  $[\text{C}_2\text{MIm}][\text{NTf}_2]$  at  $T = 303$  K. The NGKPL force field is shown in the blue line and the KPL force field in the red dashed line.

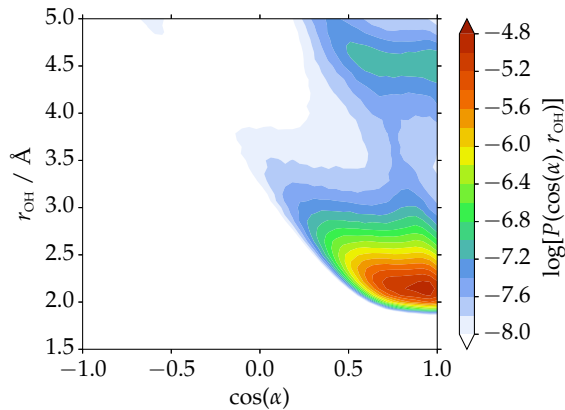


FIG. 9. Probability density of the anion-oxygens around the C(2) hydrogen sites as function of the intermolecular distance  $r_{\text{OH}}$  and the angle between the C(2)-H bond-vector and the intermolecular C(cation)-O(anion) vector. Shown for the NGKPL force field at  $T = 303$  K.

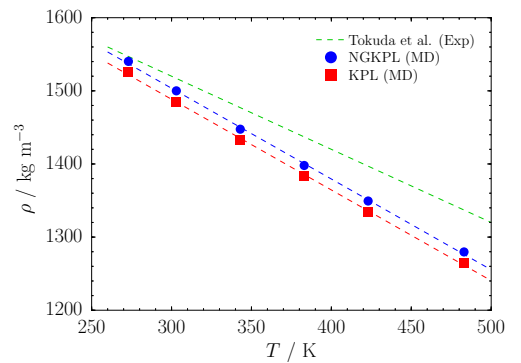


FIG. 10. Mass densities of  $[\text{C}_2\text{MIm}][\text{NTf}_2]$  as function of temperature. The experimental data of Tokuda *et al.* is given according to their fitted temperature dependence (green dashed line) [39]. The results from our molecular dynamics simulation using the NGKPL (blue dots) and KPL (red squares) force fields were fitted with a linear function represented by the dashed lines. See also Table IV.

vaporization enthalpies per mol of  $[\text{C}_n\text{MIm}][\text{NTf}_2]$  were here calculated by assuming ideal gas behavior with

$$\Delta_{\text{v}}H \approx \Delta_{\text{v}}U + RT, \quad (3)$$

which is a well justified approximation, given the low vapor pressures of ILs at low temperatures. The energy difference between the liquid and gas phases were computed via

$$\Delta_{\text{v}}U = U'_{\text{g}} - U'_{\text{l}} \quad (4)$$

where  $U'_{\text{l}}$  and  $U'_{\text{g}}$  are the internal energies per mol ion-pairs of the liquid and gas phases, respectively. To determine  $U'_{\text{g}}$  we performed gas phase simulations of individual ion-pairs without periodic boundary conditions. It has been shown in the literature that the gas phase of ionic liquids consists mostly of ion-pairs [47, 49–55] tied



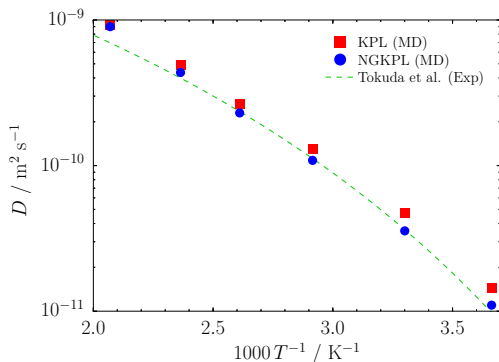


FIG. 11. Self-diffusion coefficients as function of the temperature for  $[C_2MIm][NTf_2]$ . The experimental data of Tokuda *et al.* are represented according to their fitted temperature dependence (green dashed line) [39]. The red squares (KPL) and blue dots (NGKPL) represent the results from our molecular dynamics simulations. See also Table IV.

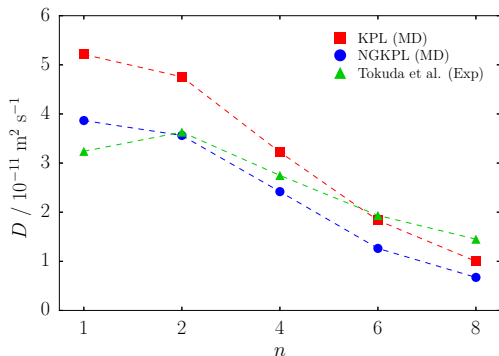


FIG. 12. Self-diffusion coefficients as a function of the alkyl chain-length for  $[C_nMIm][NTf_2]$  at  $T = 303$  K. The experimental data are shown as green triangles, the KPL force field as red squares and the NGKPL force field as blue dots. The dashed lines are only guides for the eye. See also Table V.

together by strong long-range electrostatic forces. Hence, simulating an isolated ion-pair instead of separated ions is the most realistic approximation of the IL gas phase. As it is standard practice, during the simulation of both, the liquid phase and also of the isolated ion-pair, the total linear momentum was set to zero, thus eliminating the systems center of mass translational motion. In addition, in the simulations of the isolated ion-pairs also the total angular momentum was set to zero. However, when comparing the internal energy of the gas phase and the liquid phase, we have to correct for differences in the kinetic energy stored in the translational/rotation motion

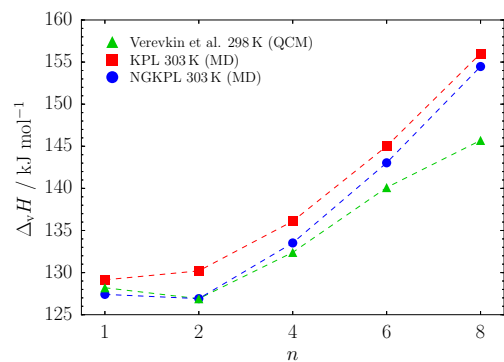


FIG. 13. Vaporization enthalpies as function of the alkyl chain-length for NGKPL (blue dots) KPL (red squares) at  $T = 303$  K. For comparison we also show the QCM data of Verevkin *et al.* for  $T = 298$  K (green triangles) [47]. See also Table V.

TABLE V. MD simulated self-diffusion coefficients of the  $[NTf_2]$  anion  $D_-$  as well as vaporization enthalpies  $\Delta_v H$  as a function of the alkyl chain-length  $n$  in  $[C_nMIm][NTf_2]$  for the KPL and the new NGKPL force field. See also Fig. 12 and Fig. 13.

$n$	$D_- / 10^{-11} \text{ m}^2 \text{ s}^{-1}$		$\Delta_v H / \text{kJ mol}^{-1}$	
	KPL	NGKPL	KPL	NGKPL
1	5.21	3.87	121.6	119.9
2	4.76	3.56	122.6	119.4
4	3.22	2.42	128.5	126.0
6	1.83	1.26	137.5	135.5
8	1.00	0.67	148.5	146.9

of either system by adding

$$U'_g = U_g + \frac{6}{2}RT \quad (5)$$

$$U'_l = U_l + \frac{3}{2}RT \times \frac{1}{N_{IP}} \quad (6)$$

per mole of ion-pairs, where  $N_{IP} = 512$  is the number of ion-pairs used in the liquid simulation, and  $U_g$  and  $U_l$  are the total energies per ion-pair as computed directly from the MD simulations. With these corrected molar internal energies  $U'_g$  and  $U'_l$  we compute the heat of vaporization  $\Delta_v H$  using Eq. 3 for a temperature of  $T = 303$  K shown in Fig. 13 and given in Table V.

Both the data computed from the KPL and from the NGKPL force field as a function of alkyl chain-length are rather close to the experimental data of Verevkin *et al.* [47]. However, we would like to point out, that the optimized NGKPL force field is in even better agreement with the QCM experiments, particularly for chain-lengths up to  $n = 4$ . Not only are the data for  $n = 2$  now in quantitative agreement with the experimental data, but also the step from  $n = 1$  to  $n = 2$  is

better captured by the new model, suggesting a significant influence of the enhanced conformational diversity of the  $[\text{NTf}_2]$  anion [56]. Since the exact slope of  $\Delta_v H$  as a function of the alkyl chain-length has been shown to be controlled by the counterbalance of electrostatic and VAN DER WAALS forces [57], the increasing deviation for longer chain-length might indicate a slight misrepresentation of size of the dispersion interaction introduced by increasing the alkyl chain-length.

### Viscosities & Reorientational Correlation Times

To further compare dynamical properties of the simulated ionic liquids with experimental data, the temperature dependence of the reorientational correlation times for the C(2)-H vector and viscosities for  $[\text{C}_2\text{MIm}][\text{NTf}_2]$  where calculated. To compare with the quadrupolar relaxation experiments of Wulf *et al.* [58] we computed reorientational correlation functions  $R(t)$  of the C(2)-H bond-vector according to

$$R(t) = \langle P_2\{\cos[\theta_{\text{CH}}(t)]\} \rangle, \quad (7)$$

where  $P_2$  is the second LEGENDRE polynomial and

$$\cos[\theta_{\text{CH}}(t)] = \frac{\vec{r}_{\text{CH}}(0) \cdot \vec{r}_{\text{CH}}(t)}{|\vec{r}_{\text{CH}}|^2} \quad (8)$$

represents the angle-cosine between the CH-bond vector at times “0” and  $t$  and  $|\vec{r}_{\text{CH}}|$  is the CH-bond length, which is kept fixed during the simulation. The reorientational correlation times  $\tau_c$  are obtained as integral over the correlation function

$$\tau_c = \int_0^\infty R(t) dt. \quad (9)$$

Here, the long-time behavior is fitted to a stretched exponential function and the total correlation time is determined by numerical integration. Again we find that both force fields are in good agreement with the experimental values, albeit with the original KPL model being slightly closer to the experimental data (see Fig. 14).

To determine the viscosities we used the approach of Zhang *et al.* [59] to compute viscosities from equilibrium-fluctuations of the off-diagonal elements of the pressure tensor via the GREEN-KUBO relation

$$\eta = \frac{V}{k_B T} \int_0^\infty \langle P_{\alpha\beta}(0) \cdot P_{\alpha\beta}(t) \rangle dt. \quad (10)$$

For each temperature we performed 15 independent  $NVT$  simulations, where the starting configurations where sampled from the earlier  $NpT$  simulations with a constant time interval of 2 ns. After a 1 ns equilibration we computed 8 ns long productions runs for each of the

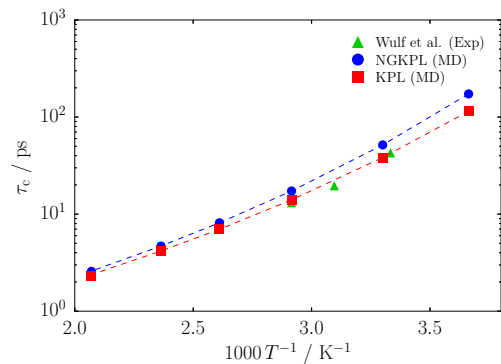


FIG. 14. Reorientational correlation time of the C(2)-H vector in  $[\text{C}_2\text{MIm}][\text{NTf}_2]$  as function of temperature. The experimental data of Wulf *et al.* [58] are shown as green triangles, KPL-data as red squares, and NGKPL-data as blue dots. The data are summarized in Table VI.

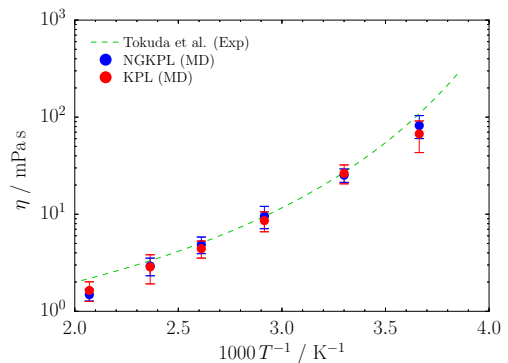


FIG. 15. Viscosities as function of temperature for  $[\text{C}_2\text{MIm}][\text{NTf}_2]$  for NGKPL (blue dots) and KPL (red squares). The experimental data was taken from Tokuda *et al.* [39]. See also Table VI.

sampled configurations storing the pressure tensor data for each time-step. Finally, the correlation function was calculated and integrated over a time-window of 1 ns for each of the 15 simulations. The average of the running integrals was calculated as well as standard deviation. The average over the running integrals as well as the standard deviation where handled as suggested by Zhang *et al.* [59] with a fitting cut off  $t_{\text{cut}}$  at the point where  $\sigma(t)$  is 40 % of the calculated average viscosity.

We find that the differences between the KPL and NGKPL models to be rather small. Both are basically lying within the statistical errors of this method. However, both force field model yield viscosities very close to the experiment (Fig. 15).



TABLE VI. Viscosities  $\eta$  and reorientational correlation times of the C(2)-H vector  $\tau_c$  as a function of temperature calculated from MD simulations of [C<sub>2</sub>MIm][NTf<sub>2</sub>] employing the KPL and the NGKPL force fields. See also Fig. 14 and Fig. 15.

$T / \text{K}$	$\eta / \text{mPa s}$		$\tau_c / \text{ps}$	
	KPL	NGKPL	KPL	NGKPL
273	$67 \pm 24$	$82 \pm 22$	173.1	114.7
303	$26 \pm 6$	$25 \pm 4$	51.6	38.2
343	$8.6 \pm 2.0$	$9.6 \pm 2.4$	17.3	14.1
383	$4.4 \pm 0.9$	$4.9 \pm 0.9$	8.1	7.0
423	$2.9 \pm 1.0$	$2.9 \pm 0.6$	4.7	4.1
483	$1.6 \pm 0.3$	$1.48 \pm 0.21$	2.6	2.3

## CONCLUSIONS

We showed that the reparametrization of the dihedral potentials as well as charges of the [NTf<sub>2</sub>] anion leads to an improvement of the force field model of Köddermann *et al.* for imidazolium based ionic liquids from 2007. The most prominent advantage of the new parameter set is that the minimum energy conformations (*trans* and *gauche*) of the anion, as demonstrated from *ab initio* calculations and RAMAN experiments, are now well reproduced.

The results obtained for [C<sub>n</sub>MIm][NTf<sub>2</sub>] show that this correction leads to a slightly better agreement between experiment and molecular dynamics simulation for a variety of properties, such as densities, diffusion coefficients, vaporization enthalpies, reorientational correlation times, and viscosities. Even though we focused on optimizing the anion parameters, the alkyl chain-length dependence is found to be general also closer to the experiment.

With this work we want to point out that it is important to re-examine established force field and, if necessary, to improve those. We highly recommend to use the new NGKPL force field for the [NTf<sub>2</sub>] anion instead of the original KPL force field. Especially for simulation aiming to describe the thermodynamics, dynamics and also structure of imidazolium based ionic liquids.

## ACKNOWLEDGEMENTS

B.G. is thankful for financial support provided by COST Action CM 1206 (EXIL - Exchange on Ionic Liquids).

\* benjamin.golub@uni-rostock.de

† jan.neumann@uni-rostock.de

‡ lisa-marie.odebrecht@uni-rostock.de

§ ralf.ludwig@uni-rostock.de

¶ dietmar.paschek@uni-rostock.de

- [1] J. N. C. Lopes, J. Deschamps, and A. A. H. Pádua, *J. Phys. Chem. B* **108**, 2038 (2004).
- [2] J. N. C. Lopes and A. A. H. Pádua, *J. Phys. Chem. B* **108**, 16893 (2004).
- [3] J. N. A. C. Lopes and A. A. H. Pádua, *J. Phys. Chem. B* **110**, 7485 (2006).
- [4] J. N. A. C. Lopes and A. A. H. Pádua, *J. Phys. Chem. B* **110**, 19586 (2006).
- [5] J. N. A. C. Lopes, A. A. H. Pádua, and K. Shimizu, *J. Phys. Chem. B* **112**, 5039 (2008).
- [6] J. N. A. C. Lopes, K. Shimizu, A. A. H. Pádua, Y. Umebayashi, S. Fukuda, K. Fujii, and S. i. Ishiguro, *J. Phys. Chem. B* **112**, 1465 (2008).
- [7] J. N. A. C. Lopes, K. Shimizu, A. A. H. Pádua, Y. Umebayashi, S. Fukuda, K. Fujii, and S. i. Ishiguro, *J. Phys. Chem. B* **112**, 9449 (2008).
- [8] T. Köddermann, K. Fumino, R. Ludwig, J. N. A. C. Lopes, and A. A. H. Pádua, *ChemPhysChem* **10**, 1181 (2009).
- [9] K. Shimizu, D. Almantariotis, M. F. C. Gomes, A. A. H. Pádua, and J. N. A. C. Lopes, *J. Phys. Chem. B* **114**, 3592 (2010).
- [10] J. N. A. C. Lopes and A. A. H. Pádua, *Theor. Chem. Acc.* **131**, 1129 (2012).
- [11] B. Guillot, *J. Mol. Liq.* **101**, 219 (2002).
- [12] P. T. Kiss and A. Baranyai, *J. Chem. Phys.* **137**, 084506 (2012).
- [13] J. F. Ouyang and R. P. Bettens, *CHIMIA* **69**, 104 (2015).
- [14] I. Shvab and R. J. Sadus, *Fluid Phase Equilib.* **407**, 7 (2015).
- [15] G. A. Cisneros, K. T. Wikfeldt, L. Ojamäe, J. Lu, X. Xu, H. Torabifard, A. P. Bartok, G. Csanyi, V. Molinero, and F. Paesani, *Chem. Rev.* **116**, 7501 (2016).
- [16] T. Köddermann, D. Paschek, and R. Ludwig, *ChemPhysChem* **8**, 2464 (2007).
- [17] D. Kerlé, R. Ludwig, A. Geiger, and D. Paschek, *J. Phys. Chem. B* **113**, 12727 (2009).
- [18] D. Kerlé, M. N. Jorabchi, R. Ludwig, S. Wohlrab, and D. Paschek, *Phys. Chem. Chem. Phys.* **19**, 1770 (2017).
- [19] R. P. Daly, J. C. Araque, and C. J. Margulis, *J. Chem. Phys.* **147**, 061102 (2017).
- [20] R. Lynden-Bell and A. J. Stone, *J. Chem. Sci.* **129**, 883 (2017).
- [21] M. M. Kazemi, M. Namboodiri, P. Donfack, A. Materny, D. Kerle, B. Rathke, and J. Kiefer, *Phys. Chem. Chem. Phys.* **19**, 15988 (2017).
- [22] K. Fujii, T. Fujimori, T. Takamuku, R. Kanzaki, Y. Umebayashi, and S. i. Ishiguro, *Journal of Physical Chemistry B Letters* **110**, 8179 (2006).
- [23] M. J. Frisch, G. W. Trucks, H. B. Schlegel, G. E. Scuseria, M. A. Robb, J. R. Cheeseman, G. Scalmani, V. Barone, B. Mennucci, G. A. Petersson, et al., *Gaussian 09 Revision D.01* (2013).
- [24] U. C. Singh and P. A. Kollman, *J. Comput. Chem.* **5**, 129 (1984).
- [25] E. Lindahl, B. Hess, and D. van der Spoel, *J. Mol. Mod.* **7**, 306 (2001).
- [26] H. J. C. Berendsen, D. van der Spoel, and R. van Drunen, *Comp. Phys. Comm.* **91**, 43 (1995).
- [27] B. Hess, C. Kutzer, D. van der Spoel, and E. Lindahl, *J. Chem. Theory Comput.* **4**, 435 (2008).

- [28] S. Pronk, S. Pall, R. Schulz, P. Larsson, P. Bjelkmar, R. Apostolov, M. R. Shirts, J. C. Smith, P. M. Kasson, D. van der Spoel, et al., *Bioinformatics* **29**, 845 (2013).
- [29] M. Abraham, B. Hess, D. van der Spoel, E. Lindahl, E. Apol, R. Apostolov, H. J. C. Berendsen, A. van Buuren, P. Bjelkmar, R. van Drunen, et al., *Gromacs 5.0.6* (2015).
- [30] U. Essmann, L. Perera, M. L. Berkowitz, T. A. Darden, H. Lee, and L. G. Pedersen, *J. Chem. Phys.* **103**, 8577 (1995).
- [31] B. Hess, H. Bekker, H. J. C. Berendsen, and J. G. E. M. Fraaije, *J. Comp. Chem.* **18**, 1463 (1997).
- [32] H. J. C. Berendsen, J. P. M. Postma, W. F. van Gunsteren, A. DiNola, and J. R. Haak, *J. Chem. Phys.* **81**, 3684 (1984).
- [33] S. Nosé, *Mol. Phys.* **52**, 255 (1984).
- [34] W. G. Hoover, *Phys. Rev. A* **31**, 1695 (1985).
- [35] M. Parrinello and A. Rahman, *J. Appl. Phys.* **52**, 7182 (1981).
- [36] S. Nosé and M. L. Klein, *Mol. Phys.* **50**, 1055 (1983).
- [37] K. Fumino, A. Wulf, and R. Ludwig, *Angew. Chem. Int. Ed.* **47**, 8731 (2008).
- [38] A. Wulf, K. Fumino, and R. Ludwig, *Angew. Chem. Int. Ed.* **49**, 449 (2010).
- [39] H. Tokuda, K. Hayamizu, K. Ishii, M. A. B. H. Susan, and M. Watanabe, *J. Phys. Chem. B* **109**, 6103 (2005).
- [40] D. H. Zaitsau, G. J. Kabo, A. A. Strechan, Y. U. Paulechka, A. Tschersich, S. P. Verevkin, and A. Heintz, *J. Phys. Chem. A* **110**, 7303 (2006).
- [41] J. P. Armstrong, C. Hurst, R. G. Jones, P. Licence, K. R. J. Lovelock, C. J. Satterley, and I. J. Villar-Garcia, *Phys. Chem. Chem. Phys.* **9**, 982 (2007).
- [42] V. N. Emel'yanenko, S. P. Verevkin, and A. Heintz, *J. Am. Chem. Soc.* **129**, 3930 (2007).
- [43] L. M. N. B. F. Santos, J. N. C. Lopes, J. A. P. Coutinho, J. M. S. S. Esperanca, L. R. Gomes, I. M. Marrucho, and L. P. N. Rebelo, *J. Am. Chem. Soc.* **129**, 284 (2007).
- [44] H. Luo, G. A. Baker, and S. Dai, *J. Phys. Chem. B Letters* **112**, 10077 (2008).
- [45] F. Heym, B. J. M. Etzold, C. Kern, and A. Jess, *Green Chem.* **13**, 1453 (2011).
- [46] M. A. A. Rocha, C. F. R. A. Lima, L. R. Gomes, B. Schröder, J. A. P. Coutinho, I. M. Marrucho, J. M. S. S. Esperanca, L. P. N. Rebelo, K. Shimizu, J. N. C. Lopes, et al., *J. Phys. Chem. B* **115**, 10919 (2011).
- [47] S. P. Verevkin, D. H. Zaitsau, V. N. Emel'yanenko, A. V. Yermalayeu, C. Schick, H. Liu, E. J. Maginn, S. Bulut, I. Krossing, and R. Kalb, *J. Phys. Chem. B* **117**, 6473 (2013).
- [48] B. Schröder and J. A. P. Coutinho, *Fluid Phase Equilib.* **370**, 24 (2014).
- [49] D. H. Zaitsau, V. Emel'yanenko, P. Stange, C. Schick, S. P. Verevkin, and R. Ludwig, *Angew. Chem. Int. Ed.* **55**, 11682 (2016).
- [50] S. P. Verevkin, D. H. Zaitsau, V. N. Emel'yanenko, and A. Heintz, *J. Phys. Chem. B* **115**, 12889 (2011).
- [51] D. H. Zaitsau, K. Fumino, V. N. Emel'yanenko, A. V. Yermalayeu, R. Ludwig, and S. P. Verevkin, *ChemPhysChem* **13**, 1868 (2012).
- [52] S. P. Verevkin, R. V. Ralys, D. H. Zaitsau, V. N. Emel'yanenko, and C. Schick, *Thermochim. Acta* **538**, 55 (2012).
- [53] M. Ahrenberg, M. Brinckmann, J. W. P. Schmelzer, M. Beck, C. Schmidt, O. Keßler, U. Kragl, S. P. Verevkin, and C. Schick, *Phys. Chem. Chem. Phys.* **16**, 2971 (2014).
- [54] S. P. Verevkin, D. H. Zaitsau, V. N. Emel'yanenko, C. Schick, S. Jayaraman, and E. J. Maginn, *Chem. Commun.* **48**, 6915 (2012).
- [55] V. N. Emel'yanenko, G. Boeck, S. P. Verevkin, and R. Ludwig, *Chem. Eur. J.* **20**, 11640 (2014).
- [56] K. Fumino, A. Wulf, S. Verevkin, A. Heintz, and R. Ludwig, *ChemPhysChem* **11**, 1623 (2010).
- [57] T. Köddermann, D. Paschek, and R. Ludwig, *ChemPhysChem* **9**, 549 (2008).
- [58] A. Wulf, R. Ludwig, P. Sasisanker, and H. Weingärtner, *Chem. Phys. Lett.* **439**, 323 (2007).
- [59] Y. Zhang, A. Otani, and E. J. Maginn, *J. Chem. Theory Comput.* **11**, 3537 (2015).